

## APPENDIX

The self-energies given in Figs. 2a and 2b can be evaluated in the usual way starting from the  $s$ -electron Green's function<sup>13</sup>

$$G_{k\sigma}^s(t-t') = -i\langle T(a_{k\sigma}(t)a_{k\sigma}^\dagger(t')S) \rangle_{\text{cont}}, \quad (\text{A1})$$

where  $\langle \rangle_{\text{cont}}$  indicates the fact that we consider only connected diagrams, and by expanding  $S$  to second order in  $V$  and  $\tilde{V}$ .

When this is done for spin  $\uparrow$   $s$  electrons we get

$$G_{k\uparrow}^s(t-t') = G_{k\uparrow}^{0s}(t-t') + V^2 \int \int G_{k\uparrow}^{0s}(t-\tau) \\ \times G_{\downarrow}^{0d}(\tau-\tau') G_{k\uparrow}^{0s}(\tau'-t') d\tau d\tau' \quad (\text{A2})$$

from which we see that

$$\Sigma^\dagger(\tau-\tau') = V^2 G_{\downarrow}^{0d}(\tau-\tau'), \quad (\text{A3})$$

<sup>13</sup> A. A. Abrikosov, L. P. Gor'kov, and I. E. Dzyaloshinski, *Methods of Quantum Field Theory in Statistical Physics* (Prentice-Hall, Inc., Englewood Cliffs, New Jersey, 1963).

using

$$G = G^0 + G^0 \Sigma G = G^0 + G^0 \Sigma G^0 + \dots, \quad (\text{A4})$$

where  $\Sigma^\dagger$  is the self-energy shown in Fig. 2a.

In a similar way, one obtains for the self-energies in Fig. 2b, reading from left to right,

$$\Sigma_1^\dagger(\tau-\tau') = V^2 G_{\downarrow}^{0d}(\tau-\tau'), \quad (\text{A5})$$

$$\Sigma_2^\dagger(\tau, \tau') = V^2 G_{\downarrow}^{0d}(\tau-\tau') f(\tau), \quad (\text{A6})$$

$$\Sigma_3^\dagger(\tau, \tau') = V^2 G_{\downarrow}^{0d}(\tau-\tau') f^*(\tau'), \quad (\text{A7})$$

$$\Sigma_4^\dagger(\tau, \tau') = V^2 G_{\downarrow}^{0d}(\tau-\tau') f(\tau) f^*(\tau'). \quad (\text{A8})$$

Adding (A5) through (A8), we obtain the total self-energy  $\Sigma^\dagger(\tau-\tau')$ :

$$\Sigma^\dagger(\tau-\tau') = V^2 G_{\downarrow}^{0d}(\tau-\tau') e^{iU(\tau'-\tau)}. \quad (\text{A9})$$

Notice that while  $\Sigma_2$ ,  $\Sigma_3$ , and  $\Sigma_4$  are functions of  $\tau$  and  $\tau'$ ,  $\Sigma^\dagger$  is a function only of  $\tau-\tau'$ .

Fourier transforming  $\Sigma^\dagger$  and  $\Sigma^\dagger$ , and taking their difference, one obtains the  $J_{\text{eff}}$  given in Eq. (23).

## Surface Structure of Clean Au (100) and Ag (100) Surfaces\*

P. W. PALMBERG<sup>†</sup> AND T. N. RHODIN

*Department of Engineering Physics, Cornell University, Ithaca, New York*

(Received 20 April 1967; revised manuscript received 22 May 1967)

The proposal that reconstructed phases may exist for the clean (100) surfaces of some fcc metals is considered in terms of results obtained from low-energy electron-diffraction studies of epitaxial single-crystal films of silver and gold grown in ultrahigh vacuum ( $1 \times 10^{-10}$  Torr). The purpose of this paper is to show that the experimentally observed (1 $\times$ 5) structure on the Au(100) surface and the (1 $\times$ 1) structure on the Ag (100) surface are characteristic of the clean surface, and to suggest a possible atomic structure for the reconstructed Au(100) surface. The evidence from the epitaxial film studies indicates the occurrence of a thin hexagonal layer of pure gold on the (100) substrate rather than an impurity-stabilized surface layer of hexagonal symmetry, of some unknown substance. It is suggested that the interfacial energy between a thin hexagonal layer and the nonreconstructed substrate may be the determining factor in the occurrence of reconstruction on the (100) surface of fcc metals.

**A**LTHOUGH it is generally assumed that clean metal surfaces are characterized by a bulk atomic arrangement, some recent experiments on Pt,<sup>1</sup> Pd,<sup>2</sup> Au,<sup>3</sup> and Ag<sup>3</sup>, suggest that reconstructed phases may exist for the clean (100) surface of some metals. There

\* Support through Air Force Office of Scientific Research Grant No. AF-AFOSR-876-56 is gratefully acknowledged.

<sup>†</sup> Present address: North American Aviation Science Center, Thousand Oaks, California.

<sup>1</sup> S. Hagstrom, H. B. Lyon, and G. A. Somorjai, *Phys. Rev. Letters* **15**, 491 (1965); see also, H. B. Lyon and G. A. Somorjai, *J. Chem. Phys.* **46**, 2539 (1967).

<sup>2</sup> H. B. Lyon, A. M. Mattera, and G. A. Somorjai, *Fundamentals of Gas-Surface Interactions*, edited by M. Rogers, H. Saltsburg, and J. N. Smith, Jr. (Academic Press Inc., New York, 1967); See also: A. M. Mattera, R. M. Goodman, and G. A. Somorjai, *Surface Science* **7**, 26 (1967).

<sup>3</sup> D. G. Fedak and N. A. Gjostein, *Phys. Rev. Letters* **16**, 171 (1966); *Acta Met.* **15**, 827 (1967).

has been considerable disagreement on whether these observed superstructures are characteristic of clean metals or whether they are stabilized by impurities. The purpose of this paper is to report on some experiments in which it is believed that contamination does not play a role and to suggest a possible atomic structure for the Au (100) surface.

One of the difficulties encountered in preparing surfaces for low-energy electron diffraction (LEED) studies is diffusion of impurities from the bulk. Even for crystals of highest available purity, bulk contamination represents an almost inexhaustible source of surface impurities unless the samples are extremely thin. One method of forming very thin crystals is to grow epitaxial films on inert substrates.

Gold and silver epitaxial films of the (100) orientation have been prepared in an ultra-high vacuum LEED system on both KCl<sup>4</sup> and MgO<sup>5</sup> substrates. In agreement with observations on bulk crystals<sup>2,3</sup> a (1×5) LEED pattern (Fig. 1) has consistently been observed for Au films grown between 100 and 300°C on both KCl and MgO. Silver films, however, always produced a (1×1) LEED pattern (Fig. 2).

It is believed that these observed structures were not influenced by impurities for the following reasons. Films approximately 500 Å thick were grown at rates up to 1 Å/sec in vacuum as low as  $2 \times 10^{-10}$  Torr on substrates cleaved in ultrahigh vacuum (UHV). Even if all impurities remained on the Au surface, simple considerations show that under these conditions, insufficient residual gas reaches the surface during film formation to influence the surface structure. Contamination from the substrate can be ruled out on the basis that the (1×5) structure has been observed on films

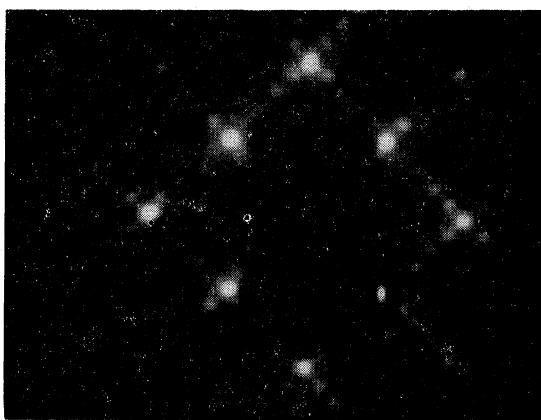


FIG. 1. (1×5) LEED pattern from (100) film grown on UHV-cleaved MgO at 200°C. 133 eV.

grown on both KCl and MgO. A final potential source of contamination is the Au flux. However, chemical analysis<sup>6</sup> by spark source mass spectroscopy and dc emission spectroscopy of the Au revealed no impurities in quantities greater than five parts in  $10^5$ . A more important examination of the Au and Ag sources was made in situ by directing the flux into an Electronics Associates, Inc. quadrupole mass spectrometer. Within the sensitivity of the measurement (one part in  $10^3$ ) no impurities were detected. On the basis of these observations it seems highly unlikely that either the Au (100) 1×5 or Ag (100) 1×1 structures were affected by impurities.

It seems relevant, therefore, to consider possible

<sup>4</sup> P. W. Palmberg, T. N. Rhodin, and C. J. Todd, *Appl. Phys. Letters* 10, 122 (1967).

<sup>5</sup> P. W. Palmberg, T. N. Rhodin, and C. J. Todd, *Appl. Phys. Letters* (to be published).

<sup>6</sup> Assistance in the analyses from the Analytical Facility of the Cornell Materials Science Center is gratefully acknowledged.

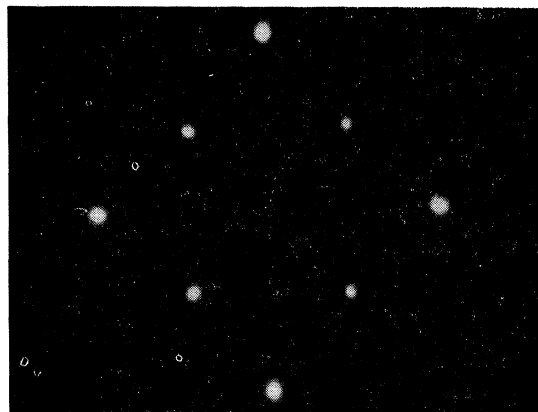


FIG. 2. (1×1) LEED pattern from (100) Ag film grown on UHV-cleaved MgO at 200°C 58 eV.

models for a clean Au (100) 1×5 structure and to discuss possible reasons for the discrepancy between Au and Ag in terms of known properties of these materials.

Fedak and Gjostein<sup>2,7</sup> have suggested that the (1×5) structure is formed by an impurity stabilized surface layer of hexagonal symmetry superimposed on the (100) substrate. Consideration of the lattice parameters involved, however, suggests that the hexagonal layer could be pure Au. A representation of a single hexagonal layer of Au on the (100) surface is shown in Fig. 3. A compression of this layer of approximately 4% in the  $\frac{1}{2}$ -order direction allows six rows of the hexagonal surface layer to fit on five rows of the substrate, resulting in a (1×5) surface structure. This compression is easily absorbed by a slight "buckling" of the surface layer due to nonsymmetrical positions on the substrate.

That a hexagonal surface layer could exist seems probable since the surface energy of the (111) surface is

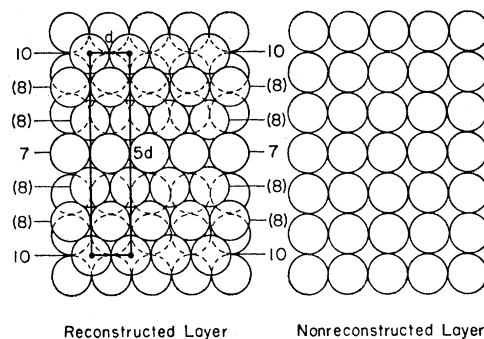


FIG. 3. Proposed atomic structure of the clean Au (100) surface. The reconstructed surface consists of a hexagonal surface layer on the nonreconstructed substrate. The numbers labeling the rows of the hexagonal layer indicate the coordination number of the corresponding surface atoms. Where the coordination number of surface atoms is not well-defined the number is enclosed in parentheses.

<sup>7</sup> D. G. Fedak and N. A. Gjostein, *Surface Science* (to be published).

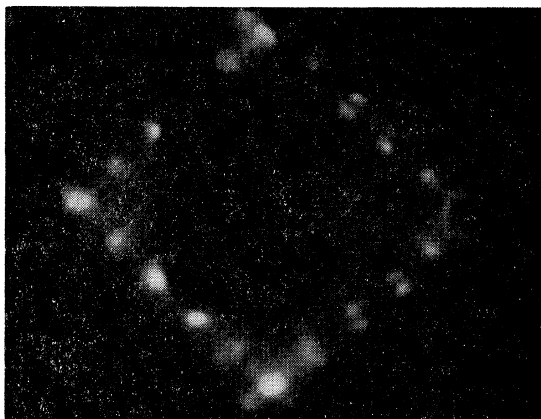


FIG. 4.  $(1 \times 5)$  LEED pattern from  $(100)$  illustrating splitting of  $\frac{1}{5}$ -order beams. The  $(00)$  beam is obscured by Au source at far right. 30 eV.

lower than that of the  $(100)$  surface. The formation of such a layer is energetically favorable provided that the difference between the  $(111)$  and  $(100)$  surface energies is greater than the interfacial energy of the hexagonal layer and the substrate. If the hexagonal surface layer is composed of more than one or two monolayers, consideration of the strain energy due to the 4% compression is necessary. Since the strain energy increases proportionally with the number of hexagonal layers, it is apparent that the hexagonal surface region must be very thin.

An attempt to determine the depth of the hexagonal surface region was made by depositing Au on a Ag  $(100)$  epitaxial film grown on MgO. Ag is an ideal substrate for this purpose because its lattice parameter closely matches that of Au. Also a superstructure was not observed on Ag so that the formation of the Au surface structure could be detected by monitoring the  $\frac{1}{5}$ -order beam intensities. In the substrate temperature range between  $-50$  and  $50^\circ\text{C}$ , it was found necessary to deposit about three monolayers of Au to form a well-ordered  $(1 \times 5)$  structure. If it is assumed that the first monolayer deposited on Ag is arranged in a square array, the hexagonal surface region must be composed of about two monolayers. Deposition of approximately one monolayer of Ag on the Au  $(100)$   $1 \times 5$  structure resulted in a simple  $(1 \times 1)$  surface structure. Hence, an apparent bulk configuration of surface atoms may result for Au crystals containing small quantities of Ag impurities.

The thermal stability of the Au  $(100)$   $1 \times 5$  structure was investigated by depositing Au on Au at substrate temperatures ranging from  $300$  to  $-200^\circ\text{C}$ . Without deposition the structure is stable through the entire temperature range. With deposition the  $(1 \times 5)$  structure was found to convert to a rather disordered  $(1 \times 1)$  structure at substrate temperatures below  $-150^\circ\text{C}$ . This transformation is believed to result because of insufficient thermal activation to form the long-range-

ordered  $(1 \times 5)$  structure. The  $(1 \times 1)$  structure thermally converts to a  $(1 \times 5)$  structure near room temperature. This transformation occurs at a somewhat lower temperature when Au is deposited simultaneously. The energy from the incident atoms is perhaps responsible for the reduction in temperature necessary for the  $(1 \times 1) \rightarrow (1 \times 5)$  structure conversion during deposition.

Fedak and Gjostein<sup>2,7</sup> have investigated the stability of the  $(1 \times 5)$  structure in the high-temperature range and found it stable up to  $800^\circ\text{C}$  where a reversible  $(1 \times 5) \rightarrow (1 \times 1)$  transformation occurs. This transformation is very likely an order-disorder conversion of the hexagonal pure Au surface region rather than of an impurity layer as postulated by Fedak and Gjostein.<sup>8</sup> At temperatures nearing the melting point patterns characteristic of  $(111)$  crystals with fiber axis orientation have also been observed.<sup>3,7</sup> These structures are formed irreversibly and are very likely contamination-stabilized as rapid diffusion of bulk impurities is expected at these extreme temperatures.<sup>2</sup> It was not possible to investigate this high-temperature region in the present experiment because of experimental limitation of the apparatus.

Fedak and Gjostein<sup>2</sup> have observed that some of the  $\frac{1}{5}$ -order beams of the Au  $(100)$   $1 \times 5$  pattern are split and have interpreted this splitting in terms of a  $(5 \times 18)$  surface unit mesh. This effect has also been observed in the present experiment (Fig. 4) and believed to be consistent with our interpretation. It is quite possible, for example, that lateral stress exists in the  $(1 \times 5)$  surface structure. This stress could be relaxed by a long-range periodic system of surface dislocations, resulting in a large surface unit mesh. However, because the splitting is small and no beams are observed other than those near the  $\frac{1}{5}$ -order positions, it must be accepted that the basic structure has dimensions closely approximating  $(1 \times 5)$  with respect to the substrate.

If one accepts the present model as valid for the Au  $(100)$  surface structure, it is interesting to consider why it exists on Au and not on Ag. The critical factor determining whether or not a hexagonal structure exists is probably the interfacial energy between the hexagonal layer and the nonreconstructed substrate. One might expect this energy to be related to the energy of bulk crystallographic imperfections. The measured bulk defect energies<sup>8-10</sup> of for example, stacking faults and twin boundaries, are extremely low for Au as well as for Ag but are not sufficiently accurately known to indicate which metal possesses the lowest defect energy. Hence, although the low-stacking fault and twin-boundary energies of Au are consistent with the present model for the Au  $(100)$   $1 \times 5$  structure, it is not clear why Au and Ag possess different  $(100)$  surface structures.

<sup>8</sup> I. L. Dillmore and R. E. Smallman, *Phil. Mag.* **12**, 191 (1965).

<sup>9</sup> G. E. Rhead and M. Mclean, *Acta Met.* **12**, 410 (1964).

<sup>10</sup> W. L. Winterbottom and N. A. Gjostein, *Acta Met.* **14**, 1041 (1966).

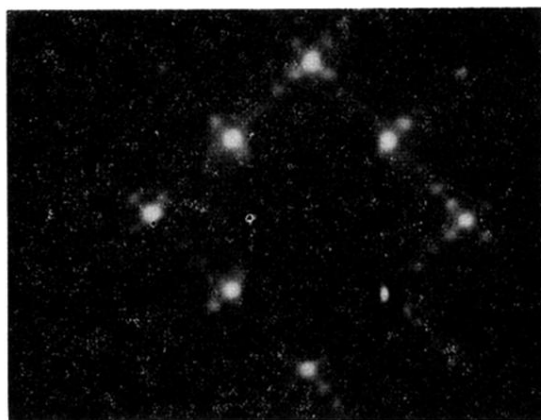


FIG. 1.  $(1 \times 5)$  LEED pattern from  $(100)$  film grown on UHV-cleaved MgO at  $200^\circ\text{C}$ . 133 eV.

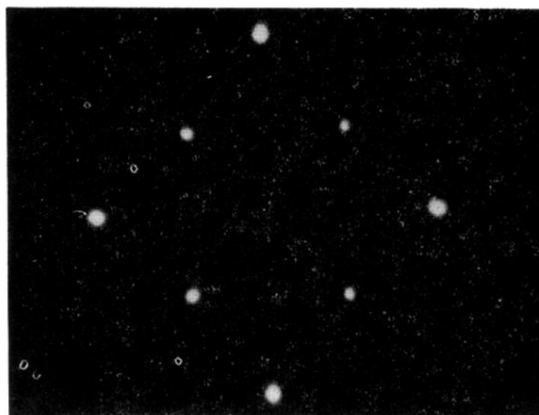


FIG. 2. (1×1) LEED pattern from (100) Ag film grown on UHV-cleaved MgO at 200°C 58 eV.

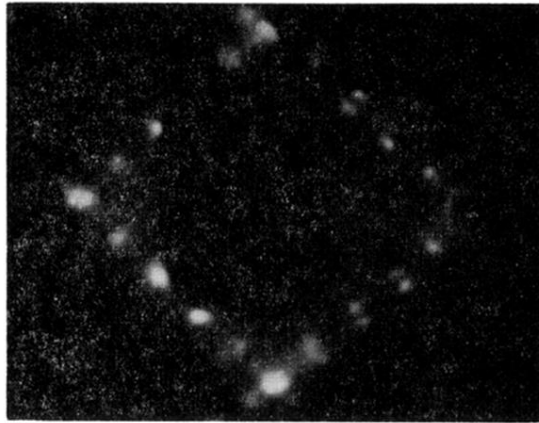


FIG. 4.  $(1 \times 5)$  LEED pattern from  $(100)$  illustrating splitting of  $\frac{1}{3}$ -order beams. The  $(00)$  beam is obscured by Au source at far right. 30 eV.